博士論文

# Mechanism and function of astrocytic calcium oscillation

（アストロサイトのカルシウム振動の発生機序と生理機能）

宇治田　早紀子

**CONTENTS**

**ABSTRACT**

Astrocytes spontaneously exhibit intracellular calcium elevations in various brain regions both in vitro and in vivo; however, neither the temporal pattern underlying the activities nor its function has been fully evaluated. Here, I utilized a long-term optical imaging technique and analyzed calcium activities of a total of more than 4,000 astrocytes in mouse hippocampal slices. Astrocytic calcium activities were largely sparse and irregular, a subset of cells exhibited calcium oscillations during which a few calcium activities repeated at a regular interval of approximately 30 s. The calcium oscillations: i) consisted of a complex reverberatory interaction between the soma and processes within astrocytes, ii) did not synchronize with other astrocytes or did not require neuronal electrical activities, iii) depended on type 2 inositol 1,4,5-trisphosphate receptors and cAMP-protein kinase A. Furthermore, this phenomenon: iv) were associated with enhanced hypertrophy in astrocytic processes, and v) were facilitated under pathological conditions, such as energy deprivation and epileptiform hyperexcitation. Therefore, it is speculated that calcium oscillations may be linked to a morphological change observed in pathological state of astrocytes. Collectively, this is the first detailed report on the mechanism and possible physiological meaning of specific temporal pattern of astrocytic calcium activity.

## INTRODUCTION

Astrocytes spontaneously exhibit various forms of intracellular calcium elevations. The calcium activities are observed in in vitro and in vivo preparations and appear in different spatiotemporal scales (Volterra et al., 2014). Increased calcium levels are implicated in the release of gliotransmitters and thereby in the modulation of cerebral blood flow (Mulligan and MacVicar, 2004; Gordon et al., 2008; Girouard et al., 2010) and neuronal activities (Jourdain et al., 2007; Henneberger et al., 2010; Navarrete and Araque, 2010; Takata et al., 2011; Min and Nevian, 2012). In pathological states, the release of gliotransmitters may cause excitotoxicity and cell death (Ding et al., 2007; Agulhon et al., 2012; Lee et al., 2013; Kawamata et al., 2014). In contrast, other reports have demonstrated that neither genetic perturbation of astrocytic calcium elevations nor gliotransmitter release from astrocytes influences synaptic transmission or blood flow (Agulhon et al., 2010; Bonder and McCarthy, 2014; Jego et al., 2014).

The reason why we lack the consensus for astrocytic function is that many previous studies have focused on calcium activities evoked artificially by electric stimulation, agonist perfusion, and photo-uncaging to evaluate the function of astrocytes (Fiacco et al., 2009; Hamilton and Attwell, 2010; Volterra et al., 2014). These evoked calcium activities may be insufficient to reproduce the natural activities of astrocytes. Indeed, a considerable proportion of the calcium activities of astrocytes are spontaneous or only weakly modulated by neuronal activity, and its generation mechanism is not completely understood. Thus, the full investigations of spontaneous calcium activities could provide a foothold in resolving the controversy regarding the function of astrocytic calcium activities.

Several studies have already revealed the spatial characteristics of spontaneous astrocytic activities (Aguado et al., 2002; Hirase et al., 2004; Kuga et al., 2011; Sasaki et al., 2011). On the other hand, the temporal patterns of spontaneous activities remain largely unknown. Moreover, little is known about the heterogeneity of activity patterns among astrocytes or the interactions of temporal patterns between astrocytes. Compared to neuronal

electrical activities, calcium activities of astrocytes are far slower; their temporal dynamics usually range from tens of seconds to minutes. Thus, the temporal modulations of astrocytic activities may be overlooked in conventional small-scale recording techniques. This notion motivated me to evaluate spontaneous calcium activities of astrocytes using a large-scale and long-term optical imaging technique. In the present work, I report a unique temporal pattern of astrocytic calcium activities, *i.e.*, cell-autonomous calcium oscillations and the physiological characteristics of this phenomenon.

## MATERIALS AND METHODS

The experiments were performed with the approval of the animal experimental ethics committee at the University of Tokyo (approval number: P24-8) according to the University of Tokyo guidelines for the care and use of laboratory animals.

*Hippocampal slice preparations*

Postnatal 9 to 12-day-old ICR mice (SLC) or type 2 inositol 1,4,5-trisphosphate receptors knockout ($IP_3R2$-KO) mice were anesthetized with ether and decapitated. The brain was immersed in ice-cold modified artificial cerebrospinal fluid (aCSF) composed of (in mM) 27 $NaHCO_3$, 1.4 $NaH_2PO_4$, 2.5 KCl, 7.0 $MgSO_4$, 1.0 $CaCl_2$, 222 sucrose, and 0.5 ascorbic acid, bubbled with 95% $O_2$ and 5% $CO_2$. Horizontal entorhino-hippocampal slices were carefully cut at a thickness of 400 μm using a vibratome. The position of the brain, the balance and speed of the blade were optimized every time to reduce unnecessary damage. All slices were cut at the speed of 0.08 mm/s. Slices were first maintained at 37°C for 20 min, and then on at room temperature in normal aCSF composed of (in mM) 127 NaCl, 26 $NaHCO_3$, 1.6 KCl, 1.24 $KH_2PO_4$, 1.3 $MgSO_4$, 2.4 $CaCl_2$, and 10 glucose.

*Calcium imaging from astrocytes*

Slices were incubated for 40 min with 0.0005% Oregon Green 488 BAPTA-1 (OGB-1) AM (Invitrogen), 0.01% Pluronic F-127 (Invitrogen), and 0.005% Cremophor EL (Sigma-Aldrich) and recovered in aCSF for >60 min. After perfusion in a recording chamber with aCSF for >10 min, spontaneous calcium signals were recorded from astrocytes in the CA1 stratum radiatum and stratum lacunosum-moleculare. Fluorophores were excited at 488 nm, and the fluorescence was captured at 1 Hz using a cooled EM-CCD camera (iXonEM+ DV897; Andor Technology) through a water-immersion objective lens (×16 or ×40, 0.8 NA, Nikon) and a Nipkow disk confocal laser scanner (CSU-10/X1; Yokogawa Electric). Slices that moved more than 3 μm in

the Z axis were discarded; those that moved in x-y dimension were *post hoc* corrected by ImageJ software (NIH) and custom-written Matlab software (Mathworks). Region of interests (ROIs) were carefully set by hand to avoid selecting non-astrocytic structures. The mean fluorescence intensity was measured from the soma of each astrocyte, and its change was defined as $\Delta F/F_0 = (F_t - F_0)/F_0$, where $F_t$ is the fluorescence intensity at time $t$, and $F_0$ is the baseline averaged for 50 s before and after time $t$. Calcium increases were semi-automatically extracted with the thresholds of 4×SD of baseline noise and a 5-s duration (Sasaki et al., 2008; Sasaki et al., 2011). The calcium activities detected were carefully inspected by eye.

*LTP induction*

LTP was induced by bipolar tungsten electrode and field EPSP was recorded by glass pipettes filled with ACSF. Both were carefully placed in the stratum radiatum of CA1 so that they are from the same distance from the pyramidal cell layer. Theta-burst stimulation protocol was used for induction (5 trains of 4 pulses at 100 Hz separated by 200 ms, repeated 6 times with 10 s inter-train interval). For test pulses, 100 μs duration pulse was given every 30s. The amplitude for test pulse and LTP induction was set at about 50% of maximum response.

*Immunohistochemistry and analysis of astrocytic morphology*

The slices were fixed either in 4% paraformaldehyde in 0.1 M phosphate buffer for 2 h or 40 mg/ml 1-ethyl-3-(3-dimethylaminopropyl)carbodiimide hydrochloride (EDC) in 0.1 M phosphate buffer solution for 3-6 h at room temperature. EDC is known to preserve calcium fluorescent dyes, such as OGB-1, inside the cell throughout the immunohistochemistry procedure (Tymianski et al., 1997). Slices fixed with paraformaldehyde were washed with PBS, whereas EDC-fixed slices were washed with 0.1 M glycine in PBS. After blocking for 60 min with 5-10% goat serum and 0.1-0.3% Triton X-100, the slices were incubated with a primary

rabbit monoclonal antibody against glial fibrillary acidic protein (GFAP; 1:500, Dako or Sigma-Aldrich) and a primary mouse monoclonal antibody against S100β (1:1000, Sigma-Aldrich) overnight at 4°C and labeled with a secondary anti-rabbit IgG Alexa-594 (1:400, Invitrogen). Sections were imaged using a confocal microscope (FV 1200; Olympus), water-immersion objective lens (×20 or ×40; Olympus) and an Ar/Kr or He-Ne laser. Super-resolution images were obtained using FV-OSR (Olympus), oil-immersion objective lens (×100; Olympus), and a laser diode.

*Application of drugs*

Tetrodotoxin (Wako), KT5720 (Sigma-Aldrich), forskolin (Sigma-Aldrich), isoproterenol (Wako), and methoxamine (Sigma-Aldrich) were bath-applied at concentrations of 1, 0.03, 50, 10, and 100 μM respectively. For treatment with tetrodotoxin and KT5720, the drugs were perfused from -5 min and throughout the recordings. Bath application was performed under fluid velocities of 3−4 ml/s. In case of treatment with 30 μM cyclopiazonic acid (Wako), slices were incubated in cyclopiazonic acid-containing aCSF for 10-15 min and then used for experiments.

*Acute pathological models*

Ischemia-like neuronal network states were induced by oxygen-glucose deprivation (OGD). Glucose in aCSF was replaced with sucrose and were continuously bubbled with 95% $N_2$ and 5% $CO_2$. Epileptic-like hyperexcitation states were induced by $Mg^{2+}$-free aCSF containing 50 μM picrotoxin (Sigma-Aldrich).

*Data analysis*

All statistical procedures were carried out by custom-written MATLAB software (Mathworks). The cell morphology was analyzed using ImageJ (National Institutes of Health). Data are reported as means ± SEMs unless otherwise specified. Paired *t*-test, Student's *t*-test, Dunnett's test, Kolmogorov-Smirnov test, and one-way repeated-measure ANOVA were performed to assess the significance of the difference. $P < 0.05$ was considered statistically significant.

## RESULTS

*Characterization of astrocytic calcium oscillations*

Functional imaging of calcium activities were conducted from 97 ± 4 astrocytes in acute hippocampal slices loaded with OGB-1-AM (Fig. 1A,B; mean ± SEM of 43 slices from 32 mice). I utilized a Nipkow-disk confocal microscope, which can rapidly scan a wide microscopic field at a low laser intensity. The laser intensity on the slice surface was set between 4−19 μW, typically 10 μW, to avoid phototoxicity (Kuga et al., 2011). The cell type was identified *post hoc* based on GFAP immunoreactivity (Fig. 1C). On average, 20.2 ± 1.3% of the astrocytes imaged were spontaneously active in 20-min control recordings ($n$ = 33 control slices). The percentage of active cells and the overall activity frequencies were constant throughout the recording time for as long as 90 min (data not shown; *e.g.*, see Fig. 2C), ruling out the possibility of ongoing damage to the slices by the imaging procedure.

In a subset of astrocytes, I discovered a characteristic pattern of oscillatory bursts, *i.e.*, oscillatory cycles of calcium activities (Fig. 2A *red dots*). Figure 2B shows a return map of the consecutive inter-activity intervals in a representative oscillatory cell, demonstrating that oscillation events (*red circles*) formed a cluster of activities and were distinct from other sporadic activities. An oscillation event was defined as a group of more than two calcium activities that repeated at an inter-activity interval of less than 60 s (Fig. 2C). On average, 4.5 ± 0.3% of the total astrocytes (34 ± 3.8% of active astrocytes) exhibited calcium oscillations (mean ± SEM of 33 slices). In any given cell, oscillation events occurred at frequencies of 0.17 ± 0.03 per hour (mean ± SEM of 3,507 cells), and in an active cell, the events occurred at frequencies of 0.80 ± 0.13 per hour (mean ± SEM of 711 cells). Among the total 2,328 calcium activities in 33 control slices, 1,012 (43%) activities constituted oscillations, whereas the remaining 57%

occurred sporadically. A single oscillation event lasted for 86.0 ± 7.0 s and consisted of 4.9 ± 0.3 calcium activities (mean ± SEM of 208 events). Compared with sporadic activities, the activities involved in calcium oscillations were significantly larger in the $\Delta F/F$ amplitude (oscillatory: 6.7 ± 0.2%, $n$ = 1,012 activities, sporadic: 6.3 ± 0.1%, $n$ = 1,316 activities; $P$ = 0.042, $t_{2326}$ = 2.03, Student's $t$-test) and were shorter in duration (oscillatory: 16.1 ± 0.39 s, sporadic: 28.2 ± 0.8 s; $P = 6.2 \times 10^{-35}$, $t_{2326}$ = 12.54, Student's $t$-test).

To examine whether oscillations occurred by chance, 1,000 surrogate datasets were generated by shuffling the calcium activities in each original dataset. More specifically, one calcium activity in a given cell was exchanged with a randomly selected activity in another randomly selected cell without changing their timings, and this activity swapping between two cells was repeated for all activities in the dataset. This procedure preserved both the activity frequencies of individual cells and the population modulation of event timings (Ikegaya et al., 2004; Sasaki et al., 2007). In all datasets, the activity-swapped surrogates contained significantly fewer oscillatory cells and oscillation events than the real datasets (Fig. 2D, $n$ = 22 datasets). Thus, the occurrence of calcium oscillations cannot be explained by chance.

One important tendency in observing calcium oscillations is that more trained experimenters observed fewer oscillations; the oscillation occurrence decreased with the training periods of astrocytic calcium imaging, reaching a plateau over three years (Fig. 3). This trend suggests that oscillations may be driven at least in part by damages to the slices. Therefore, in this work, I only employed the data acquired after training for more than three years to analyze calcium oscillations under stable experimental conditions.

Of note, the occurrence of calcium oscillation was not dependent on the postnatal day of animals (Fig. 4). Thus, the oscillation is likely not a developmental phenomenon.

*Cellular mechanisms of oscillations*

Next, I assessed the basic characteristics of oscillatory activities using pharmacologic and genetic approaches. First, consistent with previous reports (Parri et al., 2001; Nett et al., 2002), I confirmed that bath application of 1 μM tetrodotoxin did not alter either the overall activity frequency (Fig. 5A; $P = 0.41$, $t_{16} = 2.88$, Dunnett's test after one-way ANOVA; $n = 5$ slices) or sporadic activity frequency (Fig. 5B; $P = 0.56$, $t_{16} = 1.12$). In addition, tetrodotoxin did not affect either the percentage of cells that exhibited oscillations to a total of the recorded cells (Fig. 5C; $P = 0.54$, $t_{16} = 1.14$) or the frequency of oscillation events (Fig. 5D; $P = 0.43$, $t_{16} = 1.33$). Thus, astrocytic spontaneous calcium oscillations occurred independent of neuronal spiking activity.

To further assess the involvement of neuronal activity on the generation of the oscillations, I induced long-term potentiation (LTP) and recorded astrocytic calcium activity before and after LTP induction. Theta-burst stimulation on Schaffer collateral – CA1 pathway significantly increased the percentages of amplitude (Fig. 6A; $P = 6.6 \times 10^{-5}$, $t_8 = 5.39$, paired *t*-test; $n = 9$ slices) and slope (Fig. 6B; $P = 6.5 \times 10^{-5}$, $t_8 = 5.39$) of field EPSPs. LTP induction did not change either the overall activity frequency (Fig. 6C; $P = 0.68$, $t_8 = 0.42$, paired *t*-test; $n = 9$ slices) or sporadic activity frequency (Fig. 6D; $P = 0.40$, $t_8 = 0.89$). Moreover, LTP induction did not affect either the percentage of cells that exhibited oscillations to a total of the recorded cells (Fig. 6E; $P = 0.50$, $t_8 = 0.71$) or the frequency of oscillation events (Fig. 6F; $P = 0.49$, $t_8 = 0.72$). Thus, the net level of neuronal activity is not involved in the occurrence of calcium oscillations.

Astrocytes form a syncytium, interacting with adjacent cells via gap junction and gliotransmitters (Giaume et al., 2010; Giaume and Liu, 2012). To examine whether calcium oscillations emerged through astrocytic network interactions, I focused on their spatiotemporal correlations. First, I asked whether the oscillatory cells were evenly distributed and spatially

clustered. The number of oscillatory cells that were located within varying radii from a focused oscillatory cell were counted (Fig. 7A). If oscillatory cells are spatially clustered, the percentage of oscillatory cells to all cells is expected to exhibit a higher value for a smaller radius. However, the oscillatory cell probability did not change over the radii (Fig. 7B; $n$ = 156 oscillatory cells from 25 slices). The oscillatory cells seemed to be uniformly distributed in space. This analysis did not take inter-cellular temporal correlations into consideration, however. Thus, I next examined whether more closely located cells tended to oscillate simultaneously (Fig. 7C). For varying radii, I calculated the probability of cells that exhibited oscillations together with a focused oscillating cell. This oscillatory cell probability also did not change with the radii (Fig. 7D; $n$ = 104 oscillatory cells from 15 slices). Thus, calcium oscillations were unlikely to synchronize between nearby cells. These data implicate that the oscillations emerged as a single-cell-level behavior, independent of the activities of other astrocytes.

*Intracellular dynamics of calcium oscillations*

Given that the oscillations were single-cell level activities, I next focused on intracellular calcium dynamics during oscillations. I first searched oscillatory astrocytes through large-scale imaging and then observed the somata and processes from the cells using a higher magnification objective (Fig. 8A). The morphology of these subcellular structures was confirmed *post hoc* through electroporation with Alexa 594 (Reeves et al., 2011). Figure 8B shows representative line-scan plots of calcium activities along three primary processes of an astrocyte. During single oscillation events, 78 ± 25% processes exhibited calcium oscillations together with the somatic oscillatory activities (Fig. 8C; mean ± SEM of 11 cells). This ratio was higher than the ratio of processes involved in sporadic activities (Fig. 8C, $P$ = 0.03, $t_{34}$ = 1.96, Student's $t$-test). In addition, oscillation events were more frequently initiated from a process of the astrocyte than sporadic activities (Fig. 8D). During a typical oscillation event, the initial activity of one astrocytic process propagated to the soma, and subsequently, the somatic activity

propagated to more processes, constituting a Ping-Pong-like reverberation between the soma and the processes. Thus, the direction of the activity propagation was not necessarily uniform across individual cycles of an oscillation event; oscillations comprised a complex mixture of soma-to-process and process-to-soma propagations. In a few cases, local oscillations that occurred only in processes and did not propagate to the somata were observed (Fig. 8E). Such local oscillations were rare, however.

*Molecular mechanisms of calcium oscillations*

First, I investigated the calcium source of the oscillations. Calcium oscillations were completely abolished by treatment with 20 μM cyclopiazonic acid, a specific inhibitor of $Ca^{2+}$-ATPase in the endoplasmic reticulum (Fig. 9C,D; $n$ = 5 slices). Consistent with this result, calcium oscillations did not occur in slices prepared from mice lacking $IP_3R2$, a dominant type of channels that mediates intracellular calcium release in astrocytes (Sharp et al., 1999; Holtzclaw et al., 2002) (Fig. 9C,D; $n$ = 5 slices). These data indicate that the oscillations depended exclusively on $IP_3R2$-mediated calcium release. On the other hand, a few sporadic activities remained in both cyclopiazonic acid-treated slices and $IP_3R2$-KO slices (Fig. 9A,B). These calcium activities exhibited a plateau elevation (data not shown).

A variety of cells exhibit oscillatory calcium elevations that depend on $IP_3$ signal (Li et al., 1995; Mikoshiba, 2011). For instance, hepatocytes and parotid acinar cells express $IP_3R2$ and exhibit calcium oscillations, like astrocytes (Woods et al., 1986; Wojcikiewicz et al., 1994; Bruce et al., 2002). These oscillations are associated with cAMP and cAMP-dependent protein kinase (PKA) (Chatton et al., 1998; Bruce et al., 2002; Soltoff and Hedden, 2010). Therefore, I tested the involvement of the cAMP-PKA pathway in astrocytic calcium oscillations pathway using KT5720, a PKA inhibitor (Fig. 10A). Neither the frequency of the total calcium activities (Fig. 10B; $P$ = 0.20, $t_5$ = 1.48, paired $t$-test) nor the frequency of sporadic activities (Fig. 10C; $P$ = 0.61, $t_5$ = 0.55) was significantly altered by bath application of 30 nM KT5720 ($n$ = 6 slices). On the

other hand, KT5720 significantly reduced the number of cells that exhibited oscillations (Fig. 10D, $P = 0.0027$, $t_5 = 5.49$) and the frequency of oscillation events (Fig. 10E, $P = 0.024$, $t_5 = 3.20$). The $IC_{50}$ of KT5720 against PKA is 60 nM (Kase et al., 1987). KT5720 at higher than 30 nM induced swelling of slice preparations. However, the effectiveness of KT5720 at such a low concentration as 30 nM suggests that PKA activity underlies the generation of calcium oscillations.

To examine whether activation of cAMP signal is sufficient to induce calcium oscillations in astrocytes, 50 μM forskolin, an activator of adenylate cyclase, were bath-applied for 5 min (Fig. 11A). Forskolin increased the overall calcium activities of astrocytes (Fig. 11B; $P = 7.1 \times 10^{-4}$, $t_4 = 9.4$, paired *t*-test; $n = 5$ slices) and induced calcium oscillations in 47 ± 4% astrocytes (Fig. 11B; mean ± SEM of 5 slices; %cell: $P = 0.25 \times 10^{-3}$, $t_4 = 6.74$; event frequency: $P = 0.0011$, $t_4 = 8.45$, paired *t*-test). After washout, the increased calcium activities gradually returned to baseline levels until 80 min (Fig. 11A *bottom*). Astrocytes express β-adrenergic receptors (Salm and McCarthy, 1992), and their activation may increase cAMP in astrocytes through the G protein α subunit Gs. Indeed, 5-min application of 10 μM isoproterenol, a β-adrenergic receptor agonist, replicated the effect of forskolin; it induced calcium oscillations in 44 ± 6% astrocytes (Fig. 11B; mean ± SEM of 5 slices; %cell: $P = 0.97 \times 10^{-4}$, $t_4 = 8.68$; event frequency: $P = 0.0012$, $t_4 = 8.29$, paired *t*-test). Thus, both direct and endogenous receptor-mediated stimulation of cAMP-dependent pathway induced calcium oscillations. 30 nM KT5720 significantly reduced the frequency of the oscillation events (Fig. 11C; $P = 0.035$, $t_{13} = 2.66$, Dunnett's test after one-way ANOVA; $n = 5$-6 slices), whereas it did not affect the proportion of cells that exhibited calcium oscillations in response to forskolin (Fig. 11C; $P = 0.96$, $t_{13} = 0.24$). The weak effect of KT5720 on forskolin-induced calcium oscillations was perhaps due to the low concentration (30 nM), but KT5720 robustly shortened the persistence of calcium oscillations after forskolin washout (Fig. 11D). In slices prepared from $IP_3R2$-KO mice, forskolin failed to induce calcium oscillations (Fig. 11C; $n = 5$ slices).

Next, I asked whether persistent and robust calcium oscillation is a unique characteristic of cAMP activation or is a common feature of agonist activation. To test this, 100 μM methoxamine, an α-adrenergic receptor agonist was bath-applied for 5 min (Fig. 12A). Astrocytes are known to express α-adrenergic receptors (Sutin and Shao, 1992), which activate $IP_3$ - calcium pathway via G protein α subunit Gq. Methoxamine increased the overall calcium activities of astrocytes (Fig. 12B; $P = 0.011$, $t_4 = 4.52$, paired *t*-test; $n = 5$ slices) and induced calcium oscillations in astrocytes (Fig. 12B; mean ± SEM of 5 slices; %cell: $P = 7.1 \times 10^{-4}$, $t_4 = 9.42$; event frequency: $P = 0.0028$, $t_4 = 6.56$, paired *t*-test). However, the effectiveness of methoxamine to induce oscillations was weaker and transient compared to that of forskolin or isoproterenol (Fig. 12A *bottom*). Instead, methoxamine often induced plateau-type calcium elevations in astrocytes as shown in the trace in Fig. 12C *bottom*.

*Calcium oscillations as pathological correlates*

cAMP and calcium signals are both known to regulate the dynamics of cytoskeleton (Janmey, 1998) and induce a morphological change in cultured astrocytes, such as the stellation of cell bodies and the thickening of processes (Goldman and Abramson, 1990; Matsuura et al., 2002). I thus hypothesized that calcium oscillations are associated with morphological changes in astrocytes. During calcium imaging, hippocampal slices were treated with control aCSF or aCSF containing 50 μM forskolin for 5 min, fixed with paraformaldehyde after 90 min, and immunolabeled with anti-GFAP antibody (Fig. 13A). I measured the thickness of GFAP-positive primary processes that arose directly from the soma (Fig. 13B). Forskolin increased the thickness of the primary processes (Fig. 13C, non-oscillatory *versus* control: $P = 2.97 \times 10^{-6}$, $D_{177} = 0.39$; oscillatory *versus* control: $P = 1.96 \times 10^{-9}$, $D_{237} = 0.45$, Kolmogorov-Smirnov test, $n = 70$ control and 274 forskolin-treated processes). Among forskolin-treated cells, the primary processes of cells that exhibited calcium oscillations in response to forskolin were significantly thicker than those of cells that did not respond to forskolin (Fig. 13C, $P = 0.03$, $D_{274} = 0.18$, $n =$

163 oscillating and 111 non-oscillating processes). These data suggest that calcium oscillations drive forskolin-induced thickening of astrocytic processes. I did not observe significant differences in soma sizes or GFAP expression intensities between oscillatory and non-oscillatory astrocytes in forskolin-treated slices (soma size: $P = 0.42$, $D_{32} = 0.30$; GFAP intensity: $P = 0.96$, $D_{32} = 0.17$; Kolmogorov-Smirnov test; 19 oscillating and 13 non-oscillating cells).

Under pathological conditions, astrocytes become reactive and undergo morphological changes, including the thickening of processes (Sofroniew, 2009; Robel et al., 2011). Finally, I examined whether astrocytes respond to pathological stress with calcium oscillations. I treated slices with non-bubbled aCSF containing no glucose (oxygen-glucose deprivation; OGD; Fig. 14A) and $Mg^{2+}$-free aCSF containing 50 μM picrotoxin, a $GABA_A$ receptor channel inhibitor (Fig. 14B). These two aCSF conditions are used as in vitro models of cerebral ischemic states and epileptiform hyperactive states, respectively. The hyperactive states were confirmed by calcium discharges recorded from the neuropil region (Fig. 14B, *top trace*). The frequency of the total calcium activities of astrocytes was significantly increased by OGD (Fig. 14C; $P = 0.042$, $t_6 = 2.58$, $n = 7$ slices, paired *t*-test), but not by $Mg^{2+}$-free aCSF (Fig. 14C; $P = 0.10$, $t_4 = 2.11$, $n = 5$ slices). Both OGD and $Mg^{2+}$-free aCSF increased the number of oscillatory cells (Fig. 14D; OGD: $P = 0.026$, $t_6 = 2.94$; $Mg^{2+}$-free: $P = 0.032$, $t_4 = 3.22$) and the frequency of oscillation events (Fig. 14E; OGD: $P = 0.025$, $t_6 = 2.97$; $Mg^{2+}$-free: $P = 0.014$, $t_4 = 4.16$). These results, along with the dependence of calcium oscillations on the training period of experimenters (see Fig. 3), suggest that oscillatory activities of astrocytes represent an early response toward pathological states.

## DISCUSSION

In the present study, I analyzed the spatiotemporal patterns of astrocytic calcium activities in large-scale imaging datasets and discovered that a subset of astrocytes exhibited calcium oscillations. The calcium oscillations did not require neuronal activity, nor were the oscillatory cells spatially organized or temporally synchronized among astrocytes. Pharmacologic and genetic investigations revealed that calcium oscillations were dependent on $IP_3R$-mediated intracellular calcium release and PKA-dependent pathway and that activation of cAMP signal alone was sufficient to induce prolonged oscillatory activities. Calcium oscillations were correlated with thicker primary processes of astrocytes, and increased in in vitro pathological models, in which reactive gliosis is likely to be enhanced.

### *Significance of spontaneous calcium oscillations in situ*

Oscillatory calcium activity has been observed in cultured astrocytes (Charles et al., 1991; Pasti et al., 1995; Nakahara et al., 1997); however, these studies refer to the activities evoked by mechanical stimulation or agonist application. Thus, it has not been known whether astrocytes in situ exhibit different temporal patterns spontaneously at single-cell level. As far as I know, this study is first to discover and conduct detailed analysis on spontaneous temporal activity pattern in situ. I believe this was made possible by two methodological advantages, which I will describe below.

First, I chose acute hippocampal slices to observe astrocytic calcium activities. Acute slices are an experimental preparation which preserve both the cellular microenvironment including neuronal connectivity and cell morphology observed in vivo, and is a first-line choice when combining large-scale imaging and pharmacological experiments. Large-scale imaging can also be done in cultured cells. However, recent evidences show that astrocytes in culture differ from in situ astrocytes in many ways: i) gene expression and molecular profile are altered

in cultured astrocytes (Nakagawa and Schwartz, 2004; Wilhelm et al, 2004; Cahoy et al., 2008; Lovatt et al., 2007), ii) morphology of astrocytes including fine processes are lost (Matsushima et al., 2002), and iii) distinct calcium dynamics such as intercellularly propagating waves are observed (Cornell-Bell et al., 1990). Thus, cultured cells are not optimum when probing the physiological calcium activity patterns of astrocytes.

Next, the thorough analysis of calcium oscillation was not possible without large-scale imaging. As shown in Fig.1, calcium oscillation itself is spatiotemporally sparse phenomenon. In order to characterize the physiological nature of oscillation, it is necessary to recording tens of hundreds of cells simultaneously. The confocal microscopy system utilized in this study is an optimum approach in that it allows imaging from large imaging field without high laser intensity.

Whether previously studied evoked oscillatory patterns in cultured cells and the spontaneous calcium oscillations observed in this study have common molecular / functional features are unknown. However, because of the properties of cultured cells as described above, and the usage of artificial stimulations exceeding physiological levels in past studies, I believe that calcium oscillations observed in this study more likely reflect the nature of astrocytes in vivo.

*Cellular mechanisms of calcium oscillations*

The results of pharmacological and electrophysiological experiments suggest that neuronal firing or net activity level are not directly associated with the generation of calcium oscillations. Although the increase in net neuronal activity by long-term potentiation is known to increase extracellular glutamate concentration (Ikegami et al., 2014; Errington et al., 2003), this did not affect the occurrence of calcium oscillations. Furthermore, spatiotemporal analysis revealed that calcium oscillations do not synchronize or propagate among astrocytic network. Therefore, oscillations are likely single-cell dynamics that emerge independent of the states of

other cells. This is contrary to the well-described propagation of calcium waves (Dani et al., 1992; Kuga et al., 2011) or synchronization of sporadic activities in situ (Sasaki et al., 2011).

*Intracellular dynamics of calcium oscillations*

Because of a technical limitation in large-scale imaging using a low-magnification objective, calcium activities mainly in the astrocytic somata were observed. At a more microscopic level, however, I identified oscillations as a complex intercellular interaction between the somata and peripheral processes. Calcium oscillations involved more processes than sporadic activities, indicating that the influence of calcium signaling is spatially larger in oscillations. Interestingly, calcium oscillations often traveled between the soma and the processes in Ping-Pong-like manner. One molecular mechanism to explain such phenomenon is calcium-induced calcium release (CICR) at distal processes (Berridge et al., 1993), in which elevated calcium activates $IP_3$ or ryanodine receptors, stimulating further release of calcium from intracellular calcium store (See *Molecular mechanism of calcium oscillations*.). Therefore, calcium oscillation may be in part enhanced by soma – process interaction. These data, although still preliminary in part, suggest that oscillations are associated with wave-like spatial propagations of calcium activities and gradually recruit astrocytes at the whole-cell level, thereby modulating changes in gene expression or subcellular morphology, such as reactive gliosis. Independent local oscillations in the processes were also observed. Although the mechanism and function of this phenomenon is beyond the scope of this study, temporal activity patterns may be a useful parameter in understanding localized calcium dynamics. Future work will be necessary to assess the significance of subcellular calcium dynamics.

*Molecular mechanism of calcium oscillations*

Calcium oscillations have been documented in various cell types, including oocytes (Carroll and Swann, 1992), lymphatic cells (Wilson et al., 1987), and neuronal cells, such as

immature pyramidal cells and interneurons (Flint et al., 1999; Woodhall et al., 1999). Most, if not all, of these oscillations are generated by $IP_3$-dependent calcium release from the intracellular store. Several models attempt to explain how $IP_3$ signal induces oscillatory patterns, using a cAMP-calcium crosstalk (Vajanaphanich et al., 1995; Bruce et al., 2003; Siso-Nadal et al., 2009). A computational model predicts that an increase in cAMP triggers calcium oscillations at low concentrations of $IP_3$ that otherwise does not induce oscillations (Bugrim, 1999). In astrocytes, I found that the $IP_3R2$-calcium pathway mediates both sporadic and oscillatory calcium activities, whereas the cAMP-PKA pathway is specifically involved in oscillatory activities.

$IP_3$-dependent calcium elevation occurs via activation of $IP_3R$ and release of calcium from the endoplasmic reticulum. The termination of calcium release is generally thought to depend on the feedback inhibition of $IP_3R$ by calcium itself (Iino, 1990). Uptake of cytosolic calcium into intracellular stores by SERCA-type $Ca^{2+}$ - ATPases (Li et al., 1995) follows, reducing the cytosolic calcium concentration to normal state.

PKA-dependent pathway is reported to modulate the above calcium dynamics in rodent hepatocytes (Pittner and Fain, 1989), blowfly salivary glands (Schmidt et al., 2008; Fechner et al., 2013), rodent parotid acinar cells (Bruce et al., 2002; Soltoff and Hedden, 2010), rabbit interstitial cells of Cajal (Drumm et al., 2014), *etc*. In these cells, PKA is likely to directly phosphorylate $IP_3R2$ channels and enhance their sensitivity to $IP_3$ (Hajnoczky et al., 1993; Wojcikiewicz and Luo, 1998). Along with the modulation of calcium release, PKA also contributes to regulation of calcium clearance (Bruce et al., 2002). At the same time, intracellular calcium also affects cAMP concentrations (Gorbunova and Spitzer, 2002) via stimulation of adenylyl cyclase (Willoughby and Cooper, 2006) and phosphodiesterase (Bruce et al., 2003). These complex positive-feedforward interactions between the cAMP-PKA and $IP_3R2$-calcium pathways may contribute to the generation and elongation of calcium oscillations. However, the involvement of PKA-independent pathway, such as Epac cannot be ruled out (Schmidt et al., 2001; Oestreich et al., 2007). Of note, the origin of calcium triggered by cAMP remains

controversial (Grimaldi et al., 1999; Wu et al., 1999), but in this study, forskolin-induced calcium oscillations were completely abolished in $IP_3R2$ knockout mice. Therefore, the intracellular calcium store exclusively mediates cAMP-triggered calcium elevations at least in astrocytes.

Persistent calcium oscillation observed by activation of cAMP pathway was not a feature shared by Gq-GPCR activation. Rather, Gq-GPCR activation resulted in transient oscillatory pattern or plateau-type elevation. This data supports the idea that (1) Gq-GPCR and its downstream $IP_3R2$-calcium pathway has only a weak ability to generate oscillatory activity pattern when activated alone and (2) cAMP pathway enhances the calcium elevation resulting in oscillatory activity pattern, which is consistent with the computational model mentioned above (Bugrim, 1999).

As for the direct triggers of calcium oscillations, it remains to be evaluated. The possible candidates include change in extracellular ion concentration, neurotransmitters, and inflammatory factors in case of pathological calcium oscillations (Volterra and Meldolesi, 2005, Agulhon et al., 2012). Taking the computational studies and this data together, the triggers of calcium oscillations does not necessarily have to be different from that of single-peak activity. A cell may exhibit single-peak activity or multi-peak oscillation even to the same stimulation, depending on the intracellular concentration of cAMP or PKA. Otherwise, calcium oscillation may be triggered by stimulation different from single-peak activity. For example, calcium oscillation may reflect synergistic activation of cAMP and calcium pathway, likely by neuromodulators such as noradrenaline or acetylcholine, which activate both Gq-GPCRs and Gs-GPCRs expressed by astrocytes.

It should be noted that not all cells exhibit calcium oscillation, both spontaneously and by agonist application. This could be due to heterogeneity in extracellular microenvironment or intracellular signaling molecules. Both normal and reactive astrocytes are known to be heterogeneous population in morphologically, physiologically, and functionally (Anderson et

al., 2014; Zhang and Barres, 2010). Thus, there may be a population of astrocytes, in which the cAMP – calcium crosstalk is more easily activated than others. If calcium oscillation functions as an enhancer of reactive gliosis as discussed below, this population may act as a rapid responder to brain injury and pathology.

*Physiological function of calcium oscillations*

Despite a large body of literatures regarding cAMP-calcium interactions in other cell types, a limited number of studies have focused on cAMP in astrocytes. A few reports have demonstrated the involvement of a cAMP-calcium crosstalk in glycogenolysis and production of inflammatory molecules in cultured astrocytes (Hsiao et al., 2007; Juric et al., 2008; Muller et al., 2014). Using acute slices, I observed calcium oscillations in astrocytes and implicated them in hypertrophy of primary processes. The results in this study are in line with previous works alluding the involvement of calcium (Gao et al., 2013; Kanemaru et al., 2013) and cAMP (Kaneko et al., 1994; Segovia et al., 1994; Schubert et al., 2000) in GFAP expression and reactive gliosis.

I could not directly test whether calcium oscillation is a consequence or cause of morphological changes. However, the importance of calcium and cAMP in morphology of astrocytes, and regulation of gene expression by calcium oscillations of certain frequencies reported in other cell types (Gu and Spitzer, 1995; Dolmetsch et al., 1998; Li et al., 1998) support my idea that calcium oscillation enhances the morphological change as observed in this study. Our laboratory is now developing a genetical tool to manipulate astrocytic cAMP specifically, which may help give answer to this question.

Is oscillation itself important in the above described morphological changes? In other words, is sustained, plateau-type calcium elevation sufficient to induce such changes? As described above, a subset of gene expression has been shown to be sensitive to the frequency of calcium oscillation. Furthermore, constant, plateau-type calcium elevations is not sufficient to

induce efficient transcription (Dolmetsch et al., 1998; Tomida et al., 2003; Zhu et al., 2011). These data suggest that intracellular signaling pathways are sensitive to the temporal kinetics of calcium, not mere elevation of calcium concentration; however, how the oscillation itself regulates these pathways remains unsolved. There are two apparent differences between oscillatory and constant calcium elevation. First, constant calcium elevation likely results from saturation of machinery regulating intracellular calcium concentration, while in calcium oscillation, the machinery of calcium release and clearance remain operative. Second, when oscillation persists, it functions to accumulate calcium-related signaling more effectively and strongly than constant calcium elevation (Zhu et al., 2011; Salazar et al., 2008). These differences may allow calcium oscillation to exhibit specific effect on intracellular signaling pathways.

*Calcium oscillations in pathology*

As shown in this study, calcium oscillations were enhanced in two representative in vitro pathological models. cAMP-pathway-activating inflammatory molecules such as PGE2 (Denes et al., 2010), and neuromodulators such as noradrenaline and adenosine (O'Donnell et al., 2012; Pedata et al., 2001) are known to increase under pathological stress. These extracellular factors may elevate intracellular cAMP level astrocytes acutely or chronically. Data from our laboratory suggesting that neurons in epileptic model exhibit increased intracellular cAMP concentration (Nakahara et al., unpublished) supports this idea. The elevated cAMP concentration may allow the occurrence of calcium oscillation even by stimuli that normally does not induce oscillatory pattern, enhancing morphological changes in reactive gliosis.

From the data in this study, it is speculated that the observed calcium oscillation in pathological states enhance early stage of reactive gliosis including morphological changes, accelerating various inflammatory responses and formation of glial scars. However, whether

the hypertrophy of astrocytic processes directly impact the outcome of reactive gliosis is still not understood. Interestingly, the degree of hypertrophy and the severity of inflammation does not always coincide. For example, deletion of STAT3 signaling pathway attenuates hypertrophy and upregulation of GFAP and exhibits anti-inflammatory effect (Herrmann et al., 2008). On the other hand, deletion of NFκB, which also alters hypertrophy and GFAP upregulation, reduces the severity of inflammation (Brambilla et al., 2005). Given that NFκB is downstream of PKA, which was shown in this study to be involved in the generation of calcium oscillation, it is possible that calcium oscillation acts in pro-inflammatory manner; however, whether this is dependent on morphological changes or not is difficult to determine from these studies. Further experimental consideration is required to determine the direct impact of calcium oscillation and morphological changes enhanced by oscillation in the outcome of brain injury and disorders.

To my knowledge, this work is the first to propose the oscillatory pattern as a sign of pathological stress. Several animal models of neuronal diseases have revealed enhanced calcium activities (Ding et al., 2007; Takano et al., 2007; Kuchibhotla et al., 2009). However, none of these studies has addressed the temporal patterns of calcium dynamics. Therefore, it would be interesting to analyze the temporal profile of enhanced calcium activity in these animal models, and possibly observe the relationship between the occurrence of oscillatory pattern and the development and outcome of brain disorders.

*Conclusion*

This study enlightens the importance of temporal activity pattern in understanding the physiological mechanism and function of astrocytic calcium activity. Variety of activity patterns based on the complex interaction of intracellular signaling pathways may allow the realization of diverse output by astrocytes. I believe through analysis of temporal activity

pattern of astrocytes as done in this study will provide a novel viewpoint in evaluation of astrocytic physiology.

**FIGURES**

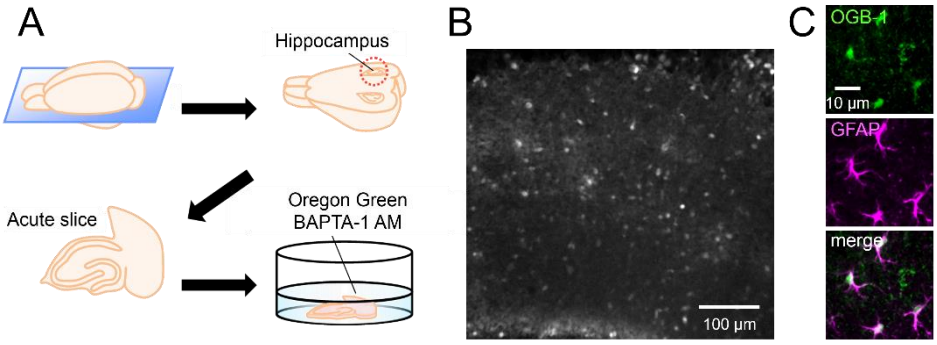


**Figure 1. In situ calcium imaging of hippocampal CA1 astrocytes.** (A) A schema showing acute hippocampal slice preparation and bulk loading of OGB-1. (B) Confocal image of an OGB-1-loaded hippocampal slice. (C) OGB-1-loaded cells were *post-hoc* immunolabeled with anti-GFAP.

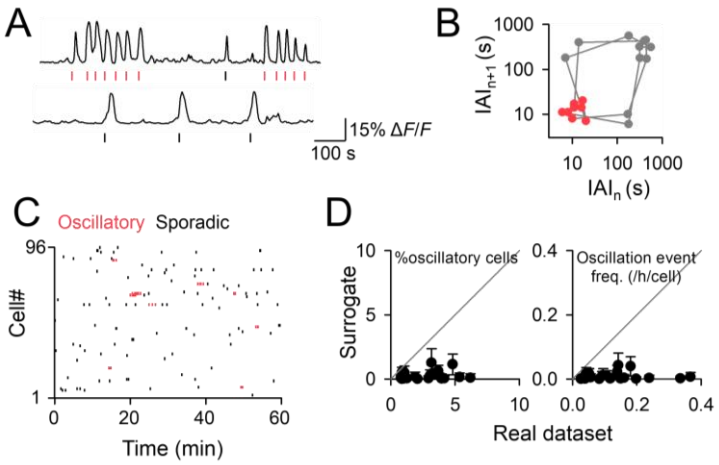


**Figure 2. Oscillations of spontaneous calcium activities in hippocampal CA1 astrocytes.** (A) Two representative Δ*F*/*F* traces showing calcium oscillations (*top*) and sporadic activities (*bottom*). Vertical bars below the traces indicate the onset times of individual calcium activities, and *red* bars correspond to oscillatory activities. (B) Representative return map of inter-activity intervals (IAIs) in a single astrocyte recorded for 60 min. The $(n+1)^{th}$ IAIs were plotted against the $n^{th}$ IAIs. *Red* circles indicate IAIs during oscillations. (C) Representative raster plot of 96 astrocytes simultaneously monitored for 60 min. Each dot indicates a single calcium activity, and *red* dots indicate oscillatory activity. (D) The percentages of oscillatory cells (*left*) to the total cells monitored and the mean frequencies of oscillation events (*right*) per cell were higher than those found in their surrogates. Each data point indicates a single dataset. The error bars represent the SDs of 1,000 surrogates. $n$ = 22 slices.

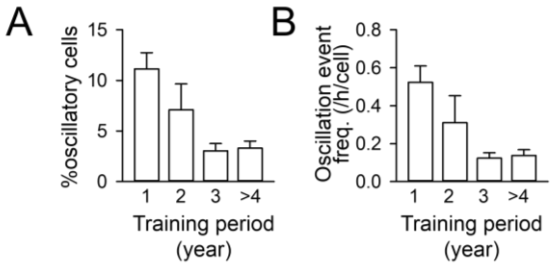


**Figure 3. Occurrence of spontaneous calcium oscillations is dependent on the training period of experimenters.** (A) The percentages of oscillatory cells to the total cells monitored are plotted as a function of training periods of experimenters. (B) The frequency of oscillation events are plotted as a function of training periods of experimenters. Error bars are SEM of 20-min recordings from a total 101 slices.

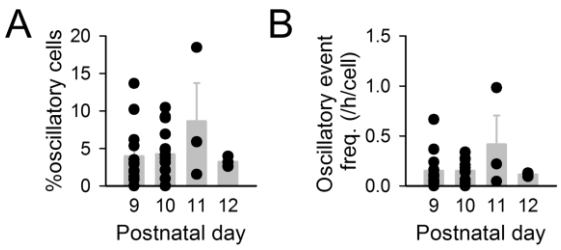


**Figure 4. Occurrence of spontaneous calcium oscillations does not depend on developmental age.** (A) The percentages of oscillatory cells to the total cells monitored are plotted as a function of postnatal day. (B) The frequency of oscillation events are plotted as a function of postnatal day. Error bars are SEM of 20-min recordings from a total 33 slices.

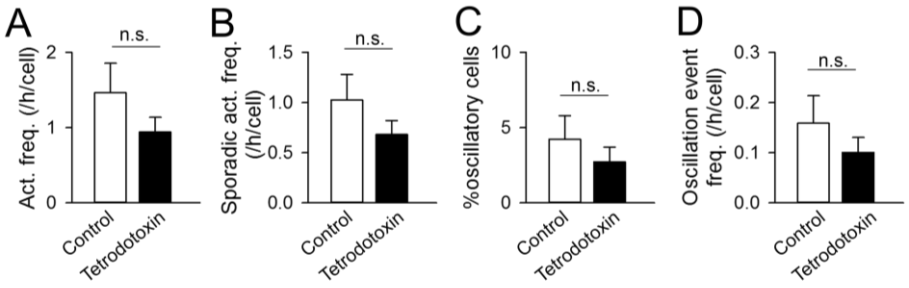


**Figure 5. Calcium oscillations are not dependent on neuronal firing.** (A-D) The frequencies of the total activities per cell (*A*), the frequencies of sporadic activities (*B*), the percentage of oscillatory cells to the total cells (*C*), the frequency of oscillation events (*D*) in control and 1 μM tetrodotoxin-treated slices. Error bars are SEM of 5 slices each.

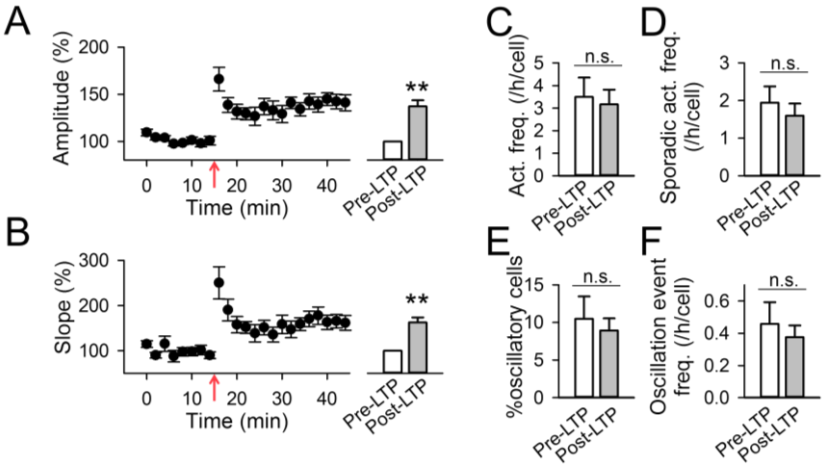


**Figure 6. Calcium oscillations are not dependent on neuronal plasticity.** (A) *Left*, the amplitude of field EPSP was plotted relative to the mean of pre-LTP. *Red* arrow indicates the time point of LTP induction. *Right*, mean amplitude before and after induction of LTP. (B) *Left*, the slope of field EPSP was plotted relative to the mean of pre-LTP. *Red* arrow indicates the time point of LTP induction. *Right*, mean slope before and after induction of LTP. (C-F) The frequencies of the total activities per cell (*C*), the frequencies of sporadic activities (*D*), the percentage of oscillatory cells to the total cells (*E*), the frequency of oscillation events (*F*) before and 40 min post-LTP. $^{**}P < 0.01$, paired *t*-test *versus* before. Error bars are SEM of 9 slices each.

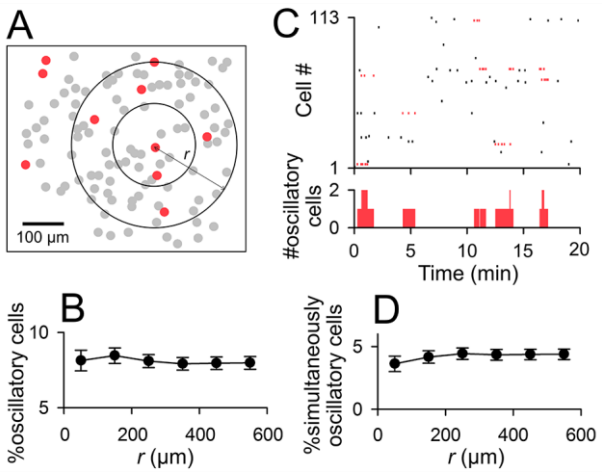


**Figure 7. Lack of inter-cellular correlations in calcium oscillations.** (A) Representative cell map of astrocytes in the CA1 stratum radiatum. Cells that exhibited oscillations are shown in *red*. (B) The percentage of oscillatory cells that were located within radii *r* from a given oscillatory cell are plotted as a function of *r*. Error bars are SEM of 156 oscillatory cells from 25 slices. (C) Oscillatory activities, indicated in *red* in the *top* raster plot, are collapsed to the *bottom* histogram of the number of oscillatory cells for a given 1-s time period. (D) The percentage of cells that exhibited calcium oscillations simultaneously with a given calcium-oscillating cell are plotted against radii (*r*) from the focused cell. Error bars are SEM of 104 oscillatory cells from 15 slices.

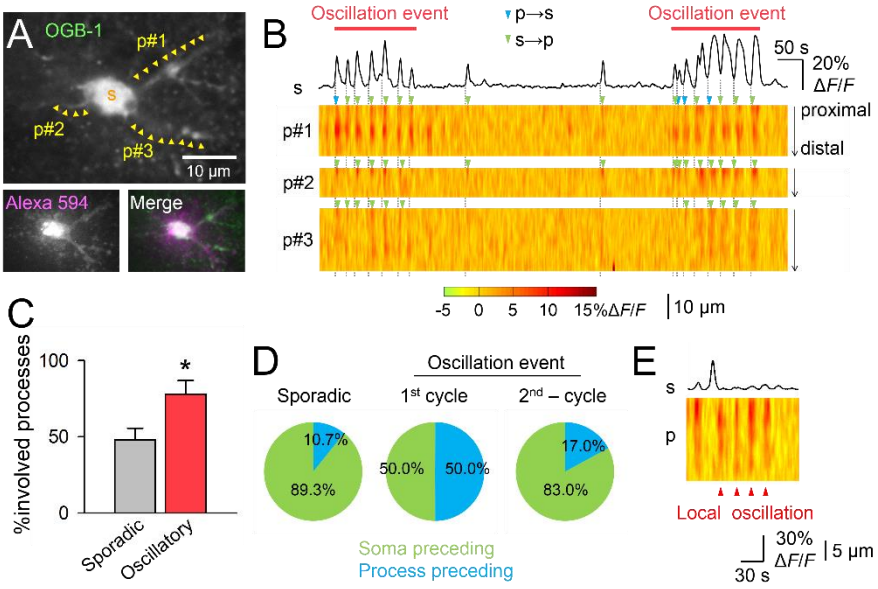


**Figure 8. Intracellular calcium dynamics during oscillations.** (A) Confocal images of an astrocyte, whose morphology was *post hoc* identified through electroporation with Alexa-Fluor 594. (B) Fluorescence changes in the soma (*top trace*) and three processes shown in *A* (*bottom XT-scans*). The dotted lines in the background indicate the onset times of the somatic calcium activities. The *green* arrowheads indicate the calcium activities propagating from the soma (*s*) to the processes (*p*), whereas the *blue* arrowheads indicate activities propagating from a process to the soma. (C) The percentages of processes exhibiting calcium activities in sporadic and oscillatory activities relative to the total number of the imaged processes. **P* = 0.03, $t_{34}$ = 1.96, Student's *t*-test. Error bars are SEM of 28 sporadic activities and 8 oscillation events in 11 astrocytes in 5 slices. (D) The ratios of soma- or process-initiated calcium activity in sporadic and oscillatory activities. *n* = 28 activities for *sporadic*, 8 activities in the *1st cycle* of the oscillations, and 47 activities in the *2nd and later cycles*. (E) Local calcium oscillations occurring in the processes (*p*), but not in the soma (*s*).

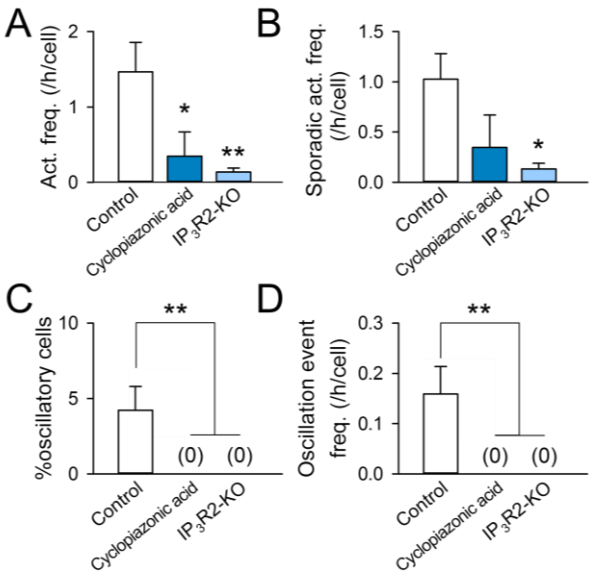


**Figure 9. Astrocytic calcium oscillations are dependent on intracellular calcium store.** (A-D) The frequencies of the total activities per cell (*A*), the frequencies of sporadic activities (*B*), the percentage of oscillatory cells to the total cells (*C*), the frequency of oscillation events (*D*) in control, 20 μM cyclopiazonic acid-treated slices and slices prepared from $IP_3R2$-KO mice. $^{**}P < 0.01$, $^{*}P < 0.05$ *versus* control, Dunnett's test after one-way ANOVA. Error bars are SEM of 5 slices each.

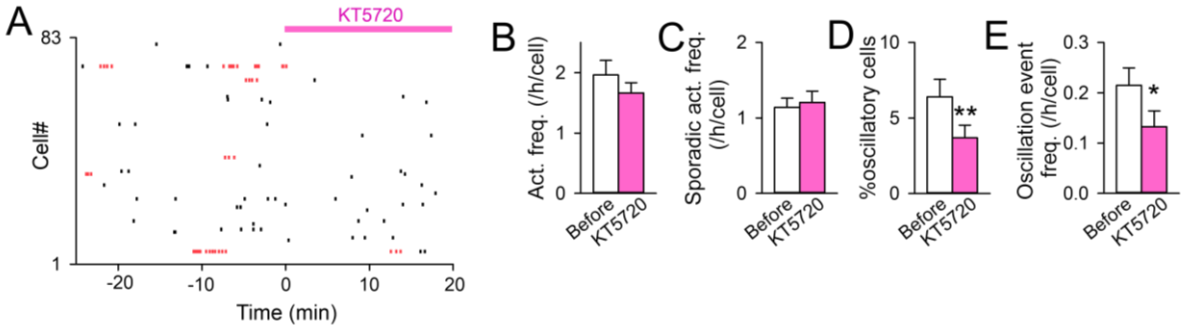


**Figure 10. PKA dependence of astrocytic calcium oscillations.** (A) Representative raster plot of spontaneous calcium activities. KT5720 was continuously bath-applied after time 0 min. *Red* dots indicate oscillations. (B-E) The frequencies of the total activities per cell (*B*), the frequencies of sporadic activities (*C*), the percentage of oscillatory cells to the total cells (*D*), and the frequency of oscillation events (*E*) before and after KT5720 treatment. **P* = 0.024, $t_5$ = 3.20, ***P* = 0.0027, $t_5$ = 5.49 *versus* before, paired *t*-test. Error bars are SEM of 6 slices.

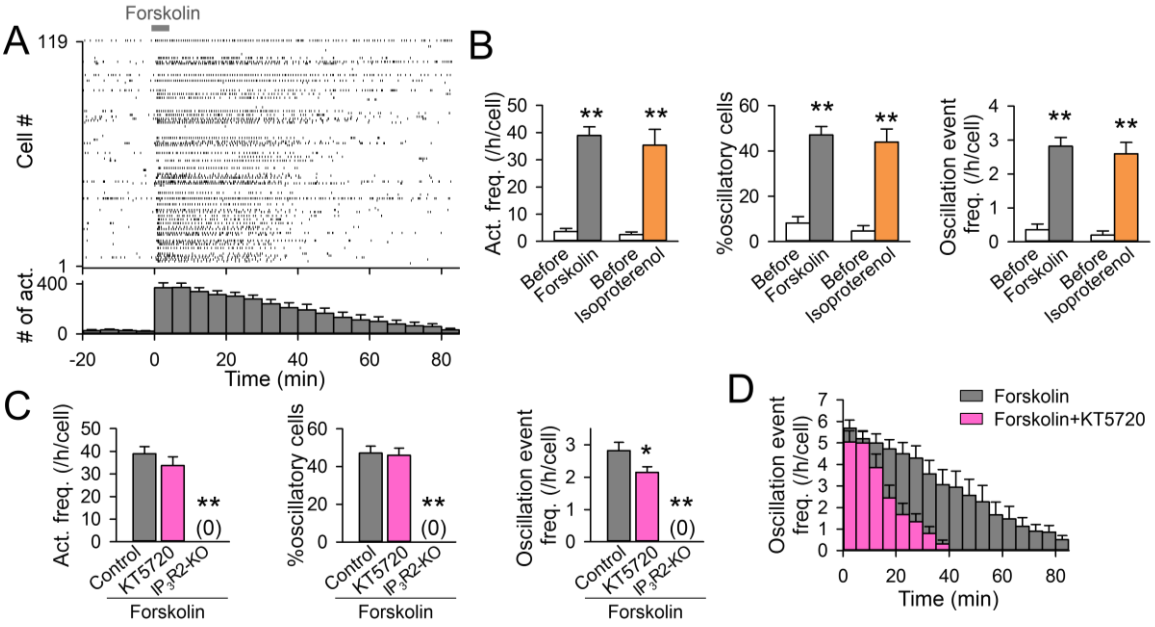


**Figure 11. cAMP induces calcium oscillations.** (A) Representative raster plot (*top*) and its time histogram (*bottom*) of calcium activities in responses to bath application of 50 μM forskolin. Forskolin was applied at time 0-5 min. (B) The frequencies of the total activities per cell (*left*), the percentage of oscillatory cells to the total cells (*middle*), and the frequency of oscillation events (*right*) are plotted 0-20 min before and 0-20 min after 5-min application of forskolin or 10 μM isoproterenol. $^{**}P < 0.01$ *versus* before, paired *t*-test. Error bars are SEM of 5 slices. (C) The same parameters as *B*, but for wild-type slices treated with forskolin alone, wild-type slices treated with forskolin under KT5720 treatment, and $IP_3R2$-KO slices treated with forskolin. $^{*}P < 0.05$, $^{**}P < 0.01$ *versus* forskolin alone, Dunnett's test after one-way ANOVA. Data were calculated for the 20-min period before and after 5-min application of forskolin. KT5720 was continuously bath-perfused throughout experiments. Error bars are SEM of 5-6 slices. (D) Time changes in the frequencies of oscillation events in response to forskolin in the absence (Forskolin) and presence of KT5720 (Forskolin+KT5720). Oscillation events were counted for every 5-min period. Data are means ± SEM of 5-6 slices.

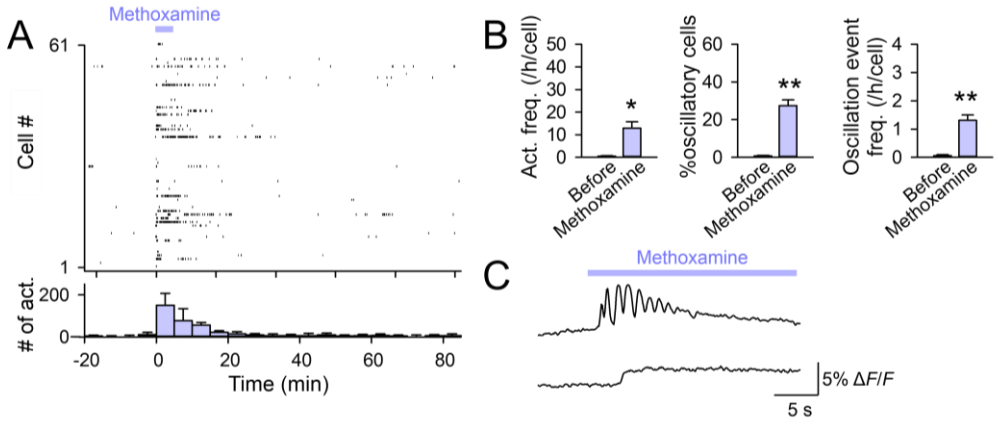


**Figure 12. Calcium elevations induced by Gq-GPCR activation.** (A) Representative raster plot (*top*) and its time histogram (*bottom*) of calcium activities in responses to bath application of 100 μM methoxamine. Methoxamine was applied at time 0-5 min. (B) The frequencies of the total activities per cell (*left*), the percentage of oscillatory cells to the total cells (*middle*), and the frequency of oscillation events per cells (*right*) are plotted 0-20 min before and 0-20 min after 5-min application of methoxamine. $^{**}P < 0.01$, $^{*}P < 0.05$ *versus* before, paired *t*-test. Error bars are SEM of 5 slices. (C) Two representative $\Delta F/F$ traces showing transient calcium oscillations (*top*) and plateau calcium elevation (*bottom*) in response to application of methoxamine.

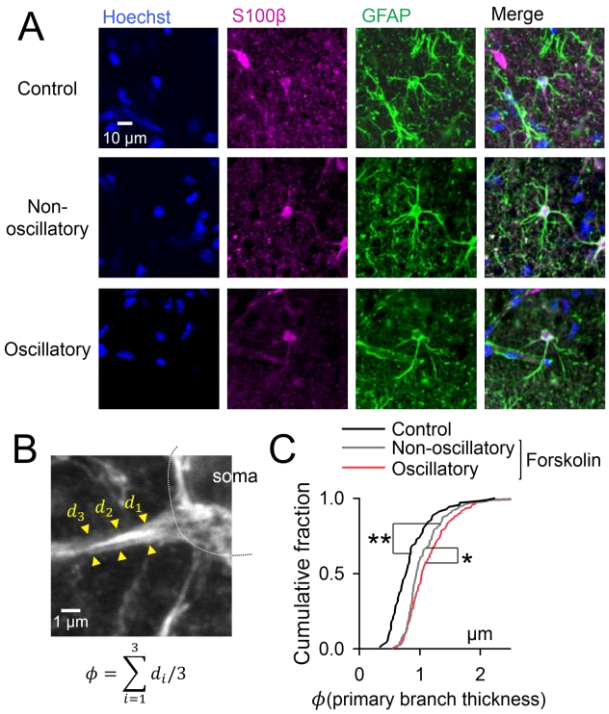


**Figure 13. Calcium oscillations are associated with severe hypertrophy of astrocytic processes.** (A) Immunohistochemical images for S100β and GFAP of control non-oscillatory cells (*top*), non-oscillatory (*middle*) and oscillatory cells (*bottom*) in response to forskolin. Hoechst was used as a counter stain of the nuclei. (B) Super-resolution confocal image showing the measurement of the thickness of an astrocytic process. For each 'primary' branch that arose directly from the soma, its thickness were averaged across three points ($d_1$, $d_2$, and $d_3$) at an interval of 1.5 μm from the soma contour (*gray line*). (C) Cumulative distributions of the primary branch thicknesses of all cells in control slices and of non-oscillatory and oscillatory cells in forskolin-treated slices. *$P$<0.05, **$P$<0.01, Kolmogorov-Smirnov test. $n$ = 70 branches from 11 cells (*control*), 111 branches from 13 cells (*non-oscillatory*), and 163 branches from 19 cells (*oscillatory*).

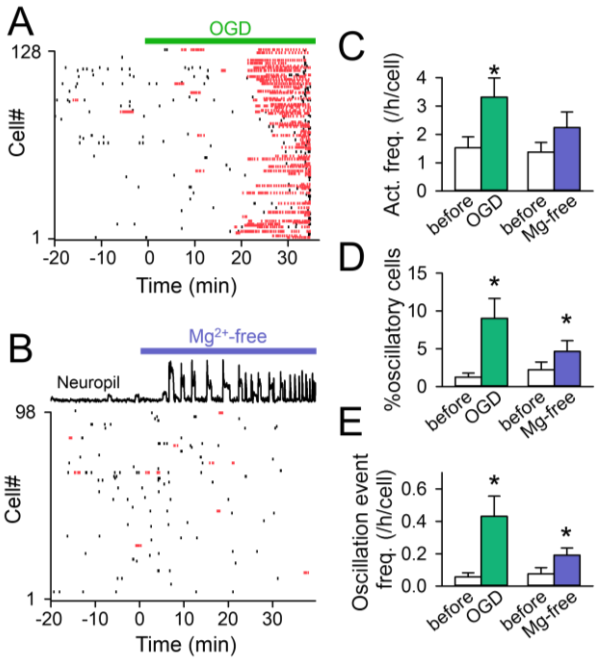


**Figure 14. Increased calcium oscillations in pathological conditions.** (A) Representative raster plot of calcium activities in responses to oxygen-glucose deprivation (OGD). OGD was conducted from time 0 min. (B) Representative raster plot of calcium activities in responses to $Mg^{2+}$-free aCSF containing 50 μM picrotoxin. Normal aCSF was changed to $Mg^{2+}$-free aCSF at time 0 min. The *top* trace is the mean calcium response of neuropil surrounding the recorded astrocytes, indicating that epileptiform neuronal discharges occurred under the disinhibited conditions. (C-E) The frequency of the total calcium activities (*C*), the percentage of oscillatory cells to the total cells (*D*), the frequency of oscillation events (*E*) before and 0-15 min after the onset of OGD or $Mg^{2+}$-free aCSF treatment. *$P < 0.05$, **$P < 0.01$ *versus* before, paired *t*-test. Error bars are SEM of 5-7 slices.

**REFERENCES**

Aguado F, Espinosa-Parrilla JF, Carmona MA, Soriano E (2002) Neuronal activity regulates correlated network properties of spontaneous calcium transients in astrocytes in situ. J Neurosci 22:9430-9444.

Agulhon C, Fiacco TA, McCarthy KD (2010) Hippocampal short- and long-term plasticity are not modulated by astrocyte Ca2+ signaling. Science 327:1250-1254.

Agulhon C, Sun MY, Murphy T, Myers T, Lauderdale K, Fiacco TA (2012) Calcium Signaling and Gliotransmission in Normal vs. Reactive Astrocytes. Front Pharmacol 3:139.

Anderson MA, Ao Y, Sofroniew MV. (2014) Heterogeneity of reactive astrocytes. Neurosci Lett 565:23-29.

Berridge MJ. Inositol trisphosphate and calcium signalling (1993) Nature 361:315-325.

Bonder DE, McCarthy KD (2014) Astrocytic Gq-GPCR-linked IP3R-dependent Ca2+ signaling does not mediate neurovascular coupling in mouse visual cortex in vivo. J Neurosci 34:13139-13150.

Brambilla R, Bracchi-Ricard V, Hu WH, Frydel B, Bramwell A, Karmally S, Green EJ, Bethea JR (2005) Inhibition of astroglial nuclear factor kappaB reduces inflammation and improves functional recovery after spinal cord injury. J Exp Med 202:145-156.

Bruce JI, Straub SV, Yule DI (2003) Crosstalk between cAMP and Ca2+ signaling in non-excitable cells. Cell Calcium 34:431-444.

Bruce JI, Shuttleworth TJ, Giovannucci DR, Yule DI (2002) Phosphorylation of inositol 1,4,5-trisphosphate receptors in parotid acinar cells. A mechanism for the synergistic effects of cAMP on Ca2+ signaling. J Biol Chem 277:1340-1348.

Bruce JI, Yule DI, Shuttleworth TJ (2002) Ca2+-dependent protein kinase--a modulation of the plasma membrane Ca2+-ATPase in parotid acinar cells. J Biol Chem 277:48172-48181.

Bugrim AE (1999) Regulation of Ca2+ release by cAMP-dependent protein kinase. A mechanism for agonist-specific calcium signaling? Cell Calcium 25:219-226.

Cahoy JD, Emery B, Kaushal A, Foo LC, Zamanian JL, Christopherson KS, Xing Y, Lubischer JL, Krieg PA, Krupenko SA, Thompson WJ, Barres BA (2008) A transcriptome database for astrocytes, neurons, and oligodendrocytes: a new resource for understanding brain development and function. J Neurosci 28:264-278.

Carroll J, Swann K (1992) Spontaneous cytosolic calcium oscillations driven by inositol trisphosphate occur during in vitro maturation of mouse oocytes. J Biol Chem 267:11196-11201.

Charles AC, Merrill JE, Dirksen ER, Sanderson MJ (1991) Intercellular signaling in glial cells: calcium waves and oscillations in response to mechanical stimulation and glutamate. Neuron 6:983-992.

Chatton JY, Cao Y, Liu H, Stucki JW (1998) Permissive role of cAMP in the oscillatory Ca2+ response to inositol 1,4,5-trisphosphate in rat hepatocytes. The Biochemical journal 330 ( Pt 3):1411-1416.

Cornell-Bell AH, Finkbeiner SM, Cooper MS, Smith SJ (1990) Glutamate induces calcium waves in cultured astrocytes: long-range glial signaling. Science 247:470–473.

Dani JW, Chernjavsky A, Smith SJ (1992) Neuronal activity triggers calcium waves in hippocampal astrocyte networks. Neuron 8:429-440.

Denes A, Thornton P, Rothwell NJ, Allan SM (2010) Inflammation and brain injury: acute cerebral ischaemia, peripheral and central inflammation. Brain Behav Immun 24:708-723.

Ding S, Fellin T, Zhu Y, Lee SY, Auberson YP, Meaney DF, Coulter DA, Carmignoto G, Haydon PG (2007) Enhanced astrocytic $Ca^{2+}$ signals contribute to neuronal excitotoxicity after status epilepticus. J Neurosci 27:10674-10684.

Dolmetsch RE, Xu K, Lewis RS (1998) Calcium oscillations increase the efficiency and specificity of gene expression. Nature 392:933-936.

Drumm BT, Sergeant GP, Hollywood MA, Thornbury KD, McHale NG, Harvey BJ (2014) The role of cAMP dependent protein kinase in modulating spontaneous intracellular $Ca^{2+}$ waves

in interstitial cells of Cajal from the rabbit urethra. Cell Calcium 56:181-187.

Errington ML, Galley PT, Bliss TVP (2003) Long-term potentiation in the dentate gyrus of the anaesthetized rat is accompanied by an increase in extracellular glutamate: real-teime measurements using a novel dialysis electrode. Philos Trans R Soc Lond B Biol Sci 358:675-687.

Fechner L, Baumann O, Walz B (2013) Activation of the cyclic AMP pathway promotes serotonin-induced $Ca^{2+}$ oscillations in salivary glands of the blowfly Calliphora vicina. Cell Calcium 53:94-101.

Fiacco TA, Agulhon C, McCarthy KD (2009) Sorting out astrocyte physiology from pharmacology. Annu Rev Pharmacol Toxicol 49:151-174.

Flint AC, Dammerman RS, Kriegstein AR (1999) Endogenous activation of metabotropic glutamate receptors in neocortical development causes neuronal calcium oscillations. Proc Natl Acad Sci U S A 96:12144-12149.

Gao K, Wang CR, Jiang F, Wong AY, Su N, Jiang JH, Chai RC, Vatcher G, Teng J, Chen J, Jiang YW, Yu AC (2013) Traumatic scratch injury in astrocytes triggers calcium influx to activate the JNK/c-Jun/AP-1 pathway and switch on GFAP expression. Glia 61:2063-2077.

Giaume C, Liu X (2012) From a glial syncytium to a more restricted and specific glial networking. J Physiol Paris 106:34-39.

Giaume C, Koulakoff A, Roux L, Holcman D, Rouach N (2010) Astroglial networks: a step further in neuroglial and gliovascular interactions. Nat Rev Neurosci 11:87-99.

Girouard H, Bonev AD, Hannah RM, Meredith A, Aldrich RW, Nelson MT (2010) Astrocytic endfoot $Ca^{2+}$ and BK channels determine both arteriolar dilation and constriction. Proc Natl Acad Sci U S A 107:3811-3816.

Goldman JE, Abramson B (1990) Cyclic AMP-induced shape changes of astrocytes are accompanied by rapid depolymerization of actin. Brain Res 528:189-196.

Gorbunova YV, Spitzer NC (2002) Dynamic interactions of cyclic AMP transients and

spontaneous $Ca^{2+}$ spikes. Nature 418:93-96.

Gordon GR, Choi HB, Rungta RL, Ellis-Davies GC, MacVicar BA (2008) Brain metabolism dictates the polarity of astrocyte control over arterioles. Nature 456:745-749.

Grimaldi M, Favit A, Alkon DL (1999) cAMP-induced cytoskeleton rearrangement increases calcium transients through the enhancement of capacitative calcium entry. J Biol Chem 274:33557-33564.

Gu X, Spitzer NC (1995) Distinct aspects of neuronal differentiation encoded by frequency of spontaneous $Ca^{2+}$ transients. Nature 375:784-787.

Hajnoczky G, Gao E, Nomura T, Hoek JB, Thomas AP (1993) Multiple mechanisms by which protein kinase A potentiates inositol 1,4,5-trisphosphate-induced $Ca^{2+}$ mobilization in permeabilized hepatocytes. The Biochemical journal 293 ( Pt 2):413-422.

Hamilton NB, Attwell D (2010) Do astrocytes really exocytose neurotransmitters? Nat Rev Neurosci 11:227-238.

Herrmann JE, Imura T, Song B, Qi J, Ao Y, Nguyen TK, Korsak RA, Takeda K, Akira S, Sofroniew MV (2008) STAT3 is a critical regulator of astrogliosis and scar formation after spinal cord injury. J Neurosci 28:7231-7243.

Henneberger C, Papouin T, Oliet SH, Rusakov DA (2010) Long-term potentiation depends on release of D-serine from astrocytes. Nature 463:232-236.

Hirase H, Qian L, Bartho P, Buzsaki G (2004) Calcium dynamics of cortical astrocytic networks in vivo. PLoS Biol 2:E96.

Holtzclaw LA, Pandhit S, Bare DJ, Mignery GA, Russell JT (2002) Astrocytes in adult rat brain express type 2 inositol 1,4,5-trisphosphate receptors. Glia 39:69-84.

Hsiao HY, Mak OT, Yang CS, Liu YP, Fang KM, Tzeng SF (2007) TNF-alpha/IFN-gamma-induced iNOS expression increased by prostaglandin E2 in rat primary astrocytes via EP2-evoked cAMP/PKA and intracellular calcium signaling. Glia 55:214-223.

Iino M (1990) Biphasic Ca2+ dependence of inositol 1,4,5-trisphosphate-induced Ca release in smooth muscle cells of the guinea pig taenia caeci. J Gen Physiol 95:1103-1122.

Ikegami Y, Hozumi S, Shoji A, Hirano-Iwata A, Bliss T, Sugawara M (2014) Real-time monitoring of extracellular L-glutamate levels released by high-frequency stimulation at region CA1 of hippocampal slices with a glass capillary-based L-glutamate sensor. Sensing Bio Res 1:31-37.

Ikegaya Y, Aaron G, Cossart R, Aronov D, Lampl I, Ferster D, Yuste R (2004) Synfire chains and cortical songs: temporal modules of cortical activity. Science 304:559-564.

Janmey PA (1998) The cytoskeleton and cell signaling: component localization and mechanical coupling. Physiol Rev 78:763-781.

Jego P, Pacheco-Torres J, Araque A, Canals S (2014) Functional MRI in mice lacking IP3-dependent calcium signaling in astrocytes. J Cereb Blood Flow Metab 34:1599-1603.

Jourdain P, Bergersen LH, Bhaukaurally K, Bezzi P, Santello M, Domercq M, Matute C, Tonello F, Gundersen V, Volterra A (2007) Glutamate exocytosis from astrocytes controls synaptic strength. Nat Neurosci 10:331-339.

Juric DM, Loncar D, Carman-Krzan M (2008) Noradrenergic stimulation of BDNF synthesis in astrocytes: mediation via alpha1- and beta1/beta2-adrenergic receptors. Neurochem Int 52:297-306.

Kaneko R, Hagiwara N, Leader K, Sueoka N (1994) Glial-specific cAMP response of the glial fibrillary acidic protein gene cell lines. Proc Natl Acad Sci U S A 91:4529-4533.

Kanemaru K, Kubota J, Sekiya H, Hirose K, Okubo Y, Iino M (2013) Calcium-dependent N-cadherin up-regulation mediates reactive astrogliosis and neuroprotection after brain injury. Proc Natl Acad Sci U S A 110:11612-11617.

Kase H, Iwahashi K, Nakanishi S, Matsuda Y, Yamada K, Takahashi M, Murakata C, Sato A, Kaneko M (1987) K-252 compounds, novel and potent inhibitors of protein kinase C and cyclic nucleotide-dependent protein kinases. Biochem Biophys Res Commun 142:436-440.

Kawamata H, Ng SK, Diaz N, Burstein S, Morel L, Osgood A, Sider B, Higashimori H, Haydon PG, Manfredi G, Yang Y (2014) Abnormal intracellular calcium signaling and SNARE-dependent exocytosis contributes to SOD1G93A astrocyte-mediated toxicity in amyotrophic lateral sclerosis. J Neurosci 34:2331-2348.

Kuchibhotla KV, Lattarulo CR, Hyman BT, Bacskai BJ (2009) Synchronous hyperactivity and intercellular calcium waves in astrocytes in Alzheimer mice. Science 323:1211-1215.

Kuga N, Sasaki T, Takahara Y, Matsuki N, Ikegaya Y (2011) Large-scale calcium waves traveling through astrocytic networks in vivo. J Neurosci 31:2607-2614.

Lee W, Reyes RC, Gottipati MK, Lewis K, Lesort M, Parpura V, Gray M (2013) Enhanced $Ca^{2+}$-dependent glutamate release from astrocytes of the BACHD Huntington's disease mouse model. Neurobiol Dis 58:192-199.

Li YX, Keizer J, Stojilkovic SS, Rinzel J (1995) $Ca^{2+}$ excitability of the ER membrane: an explanation for IP3-induced $Ca^{2+}$ oscillations. Am J Physiol 269:C1079-1092.

Li W, Llopis J, Whitney M, Zlokarnik G, Tsien RY (1998) Cell-permeant caged InsP3 ester shows that $Ca^{2+}$ spike frequency can optimize gene expression. Nature 392:936-941.

Lovatt D, Sonnewald U, Waagepetersen HS, Schousboe A, He W, Lin JH, Han X, Takano T, Wang S, Sim FJ, Goldman SA, Nedergaard M. (2007) The transcriptome and metabolic gene signature of protoplasmic astrocytes in the adult murine cortex. J Neurosci 27:12255-12266.

Matsuura S, Ikegaya Y, Yamada MK, Nishiyama N, Matsuki N (2002) Endothelin downregulates the glutamate transporter GLAST in cAMP-differentiated astrocytes in vitro. Glia 37:178-182.

Mikoshiba K (2011) Role of IP(3) receptor in development. Cell Calcium 49:331-340.

Min R, Nevian T (2012) Astrocyte signaling controls spike timing-dependent depression at neocortical synapses. Nat Neurosci 15:746-753.

Muller MS, Fox R, Schousboe A, Waagepetersen HS, Bak LK (2014) Astrocyte glycogenolysis

is triggered by store-operated calcium entry and provides metabolic energy for cellular calcium homeostasis. Glia 62:526-534.

Mulligan SJ, MacVicar BA (2004) Calcium transients in astrocyte endfeet cause cerebrovascular constrictions. Nature 431:195-199.

Nakagawa T, Schwartz JP (2004) Gene expression patterns in in vivo normal adult astrocytes compared with cultured neonatal and normal adult astrocytes. Neurochem Int 45:203-242.

Nakahara K, Okada M, Nakanishi S (1997) The metabotropic glutamate receptor mGluR5 induces calcium oscillations in cultured astrocytes via protein kinase C phosphorylation. J Neurochem 69:1467-1475.

Navarrete M, Araque A (2010) Endocannabinoids potentiate synaptic transmission through stimulation of astrocytes. Neuron 68:113-126.

Nett WJ, Oloff SH, McCarthy KD (2002) Hippocampal astrocytes in situ exhibit calcium oscillations that occur independent of neuronal activity. Journal of Neurophysiology 87:528-537.

O'Donnell J, Zeppenfeld D, McConnell E, Pena S, Nedergaard M (2012) Norepinephrine: a neuromodulator that boosts the function of multiple cell types to optimize CNS performance. Neurochem Res 37:2496-2512.

Oestreich EA, Wang H, Malik S, Kaproth-Joslin KA, Blaxall BC, Kelley GG, Dirksen RT, Smrcka AV (2007) Epac-mediated activation of phospholipase C(epsilon) plays a critical role in beta-adrenergic receptor-dependent enhancement of $Ca^{2+}$ mobilization in cardiac myocytes. J Biol Chem 282:5488-5495.

Parri HR, Gould TM, Crunelli V (2001) Spontaneous astrocytic $Ca^{2+}$ oscillations in situ drive NMDAR-mediated neuronal excitation. Nat Neurosci 4:803-812.

Pasti L, Pozzan T, Carmignoto G. (1995) Long-lasting changes of calcium oscillations in astrocytes. J Biol Chem 270:15203-15210.

Pedata F, Corsi C, Melani A, Bordoni F, Latini S (2001) Adenosine extracellular brain

concentrations and role of A2A receptors in ischemia. Ann N Y Acad Sci 939:74-84.

Pittner RA, Fain JN (1989) Exposure of cultured hepatocytes to cyclic AMP enhances the vasopressin-mediated stimulation of inositol phosphate production. The Biochemical journal 257:455-460.

Reeves AM, Shigetomi E, Khakh BS (2011) Bulk loading of calcium indicator dyes to study astrocyte physiology: key limitations and improvements using morphological maps. J Neurosci 31:9353-9358.

Robel S, Berninger B, Gotz M (2011) The stem cell potential of glia: lessons from reactive gliosis. Nat Rev Neurosci 12:88-104.

Salazar C, Politi AZ, Höfer T (2008) Decoding of calcium oscillations by phosphorylation cycles: analytic results. Biophys J 94:1203-1215.

Salm AK, McCarthy KD (1992) The evidence for astrocytes as a target for central noradrenergic activity: expression of adrenergic receptors. Brain Res Bull 29:265-275.

Sasaki T, Matsuki N, Ikegaya Y (2007) Metastability of active CA3 networks. J Neurosci 27:517-528.

Sasaki T, Takahashi N, Matsuki N, Ikegaya Y (2008) Fast and accurate detection of action potentials from somatic calcium fluctuations. J Neurophysiol 100:1668-1676.

Sasaki T, Kuga N, Namiki S, Matsuki N, Ikegaya Y (2011) Locally synchronized astrocytes. Cerebral Cortex 21:1889-1900.

Schmidt M, Evellin S, Weernink PA, von Dorp F, Rehmann H, Lomasney JW, Jakobs KH (2001) A new phospholipase-C-calcium signalling pathway mediated by cyclic AMP and a Rap GTPase. Nature cell biology 3:1020-1024.

Schmidt R, Baumann O, Walz B (2008) cAMP potentiates InsP3-induced $Ca^{2+}$ release from the endoplasmic reticulum in blowfly salivary glands. BMC physiology 8:10.

Schubert P, Morino T, Miyazaki H, Ogata T, Nakamura Y, Marchini C, Ferroni S (2000) Cascading glia reactions: a common pathomechanism and its differentiated control by cyclic

nucleotide signaling. Ann N Y Acad Sci 903:24-33.

Segovia J, Lawless GM, Tillakaratne NJ, Brenner M, Tobin AJ (1994) Cyclic AMP decreases the expression of a neuronal marker (GAD67) and increases the expression of an astroglial marker (GFAP) in C6 cells. J Neurochem 63:1218-1225.

Sharp AH, Nucifora FC, Jr., Blondel O, Sheppard CA, Zhang C, Snyder SH, Russell JT, Ryugo DK, Ross CA (1999) Differential cellular expression of isoforms of inositol 1,4,5-triphosphate receptors in neurons and glia in brain. J Comp Neurol 406:207-220.

Siso-Nadal F, Fox JJ, Laporte SA, Hebert TE, Swain PS (2009) Cross-talk between signaling pathways can generate robust oscillations in calcium and cAMP. PLoS One 4:e7189.

Sofroniew MV (2009) Molecular dissection of reactive astrogliosis and glial scar formation. Trends Neurosci 32:638-647.

Soltoff SP, Hedden L (2010) Isoproterenol and cAMP block ERK phosphorylation and enhance [$Ca^{2+}$]i increases and oxygen consumption by muscarinic receptor stimulation in rat parotid and submandibular acinar cells. J Biol Chem 285:13337-13348.

Sutin EL, Shao Y (1992) Resting and reactive astrocytes express adrenergic receptors in the adult rat brain. Brain Res Bull 29:277-284.

Takano T, Han X, Deane R, Zlokovic B, Nedergaard M (2007) Two-photon imaging of astrocytic $Ca^{2+}$ signaling and the microvasculature in experimental mice models of Alzheimer's disease. Ann N Y Acad Sci 1097:40-50.

Takata N, Mishima T, Hisatsune C, Nagai T, Ebisui E, Mikoshiba K, Hirase H (2011) Astrocyte calcium signaling transforms cholinergic modulation to cortical plasticity in vivo. J Neurosci 31:18155-18165.

Tomida T, Hirose K, Takizawa A, Shibasaki F, Iino M (2003) NFAT functions as a working memory of Ca2+ signals in decoding Ca2+ oscillation. EMBO J 22:3825-3832.

Tymianski M, Bernstein GM, Abdel-Hamid KM, Sattler R, Velumian A, Carlen PL, Razavi H, Jones OT (1997) A novel use for a carbodiimide compound for the fixation of fluorescent

and non-fluorescent calcium indicators in situ following physiological experiments. Cell Calcium 21:175-183.

Vajanaphanich M, Schultz C, Tsien RY, Traynor-Kaplan AE, Pandol SJ, Barrett KE (1995) Cross-talk between calcium and cAMP-dependent intracellular signaling pathways. Implications for synergistic secretion in T84 colonic epithelial cells and rat pancreatic acinar cells. The Journal of clinical investigation 96:386-393.

Volterra A, Liaudet N, Savtchouk I (2014) Astrocyte $Ca^{2+}$ signalling: an unexpected complexity. Nat Rev Neurosci 15:327-335.

Volterra A, Meldolesi J (2005) Astrocytes, from brain glue to communication elements: the revolution continues. Nat Rev Neurosci 6:626-640.

Wilhelm A, Volknandt W, Langer D, Nolte C, Kettenmann H, Zimmermann H (2004) Localization of SNARE proteins and secretory organelle proteins in astrocytes in vitro and in situ. Neurosci Res 48:249-257.

Willoughby D, Cooper DM (2006) $Ca^{2+}$ stimulation of adenylyl cyclase generates dynamic oscillations in cyclic AMP. J Cell Sci 119:828-836.

Wilson HA, Greenblatt D, Poenie M, Finkelman FD, Tsien RY (1987) Crosslinkage of B lymphocyte surface immunoglobulin by anti-Ig or antigen induces prolonged oscillation of intracellular ionized calcium. J Exp Med 166:601-606.

Wojcikiewicz RJ, Luo SG (1998) Phosphorylation of inositol 1,4,5-trisphosphate receptors by cAMP-dependent protein kinase. Type I, II, and III receptors are differentially susceptible to phosphorylation and are phosphorylated in intact cells. J Biol Chem 273:5670-5677.

Wojcikiewicz RJ, Furuichi T, Nakade S, Mikoshiba K, Nahorski SR (1994) Muscarinic receptor activation down-regulates the type I inositol 1,4,5-trisphosphate receptor by accelerating its degradation. J Biol Chem 269:7963-7969.

Woodhall G, Gee CE, Robitaille R, Lacaille JC (1999) Membrane potential and intracellular Ca2+ oscillations activated by mGluRs in hippocampal stratum oriens/alveus interneurons. J

Neurophysiol 81:371-382.

Woods NM, Cuthbertson KS, Cobbold PH (1986) Repetitive transient rises in cytoplasmic free calcium in hormone-stimulated hepatocytes. Nature 319:600-602.

Wu ML, Chen WH, Liu IH, Tseng CD, Wang SM (1999) A novel effect of cyclic AMP on capacitative $Ca^{2+}$ entry in cultured rat cerebellar astrocytes. J Neurochem 73:1318-1328.

Zhang Y, Barres BA. (2010) Astrocyte heterogeneity: an underappreciated topic in neurobiology. Curr Opin Neurobiol 20:588-594.

Zhu L, Song S, Pi Y, Yu Y, She W, Ye H, Su Y, Hu Q (2011) Cumulated $Ca2^{+}$ spike duration underlies $Ca2^{+}$ oscillation frequency-regulated NFκB transcriptional activity. J Cell Sci 124:2591-2601.

**ACKNOWLEDGEMENTS**

I would like to thank my PhD advisor, Prof. Yuji Ikegaya for providing thorough support and education through five years of doctoral course. His creativity, power of expression, and zest for research has always been the greatest stimulation in pursuing my study.

I am grateful to Dr. Norio Matsuki for his kind mentorship and encouragement whenever I felt lost or unconfident. His questions and comments at the seminars were always ingoing and have given me many hints to my research.

I thank Dr. Ryuta Koyama for giving me an opportunity to work with him as a collaborator, and showing me what a true scientist should be on daily basis. His passion for pathological research has encouraged me both as a scientist and as a patient's family.

I thank Dr. Hiroshi Nomura, who has given me advice when in need, which were rational and optimistic at the same time.

My pursuit in astrocytic study has not been possible by Dr. Takuya Sasaki, from whom I learned the basics of astrocytic knowledge and ways of thinking. He introduced me to scientific community where I was able to meet wonderful glia scientists and learn many things as a scientist.

I sincerely thank Prof. Katsuhiko Mikoshiba for providing $IP_3R2$-KO transgenic mice, without which I could not finish this work.

I would like to thank my thesis committee: Prof. Kazuhisa Sekimizu, Prof. Taisuke Tomita, Prof. Takeshi Iwatsubo, Prof. Hidenori Ichijo.

I would like to express my gratitude to following glia scientists for providing me with wonderful experience of learning glial science : Dr. Kenji Tanaka, Dr. Ko Matsui, Dr. Norio Takata, Dr. Kazunori Kanemaru and Dr. Hiroko Ikeshima.

I would like to thank: Naoya Takahashi, my Shisho, for teaching me basic experimental skills and always being there as an advisor of academic life; Mika Mizunuma for encouraging me and being my role model as a tough and talented woman; Genki Minamisawa, for

introducing me to the joy of savatte and always showing me the right way as a person.

My one and only colleague in PhD course, Natsuko Imamura-Hitora has always encouraged me and helped me out countless times. I don’t know how to thank her enough. I have always respected her attitude towards her work (and private life ☺).

Akiko Asada has always been a light in my lab life. Her curiosity and brightness has helped me through tough times. Being the only astrocyte group in the lab, discussions with her has been a great stimulation and motivation.

I would like to thank Kenta Funayama, Hiroaki Norimoto, Chiaki Kobayashi, Nobuyoshi Matsumoto, Yuuki Miura, Daisuke Nakayama for supporting me both emotionally and academically and sharing countless fun times together.

I also thank Tetsuya Sakaguchi, Tomoe Ishikawa, Reimi Abe, Takeyuki Miyawaki, Kazuki Okamoto, Ryota Nakayama for all the fun discussions and daily conversations.

I am grateful to all the other members of the lab, who made five years of my lab life so enjoyable: Junya Ichikawa, Haruka Yamamoto, Atsushi Usami, Soichiro Nakahara, Huilian Shen, Kentaro Tao, Mari Sajo, Koichi Hashikawa, Megumi Seki, Mayuko Miura, Ayako Nonaka, Daisuke Ishikawa, Daisuke Miyamoto, Yoshiko Yamasaki, Yuji Takahara, Naoko Homma, Emi Shimizu, Hiroshi Shimagami, Fumitaka Masuda, Saori Okada, Hiroko Osamura, Kazuki Shibata, Hikaru Igarashi, Masamitsu Naka, Kosuke Miyajima, Masataka Ishizuka, Emi Tomikawa, Hirokazu Iwata, Zohal Baraki, Koshiro Hara, Kosuke Onoue, Tomoya Kitagawa, Chie Teshirogi, Kohei Morishita, Zhiwen Zhou, Hideki Ueda, Yusuke Watanabe, Hiroki Sugiyama, Nariaki Uemura, Satoshi, Iwasaki, Kenichi Makino, Mami Okada, Hiroto Kojima, Cong Lao, Xuezhu Sun, Hideyoshi Igata.

Most importantly, I would like to thank my family, Akifumi Ujita, Yumiko Ujita, Kanako Ujita, Akira Ujita, and Takeshi Toyoda, who have always backed me up throughout the years.